Arabian Journal of Geosciences (2021) 14:380
https://doi.org/10.1007/s12517-021-06767-3

ORIGINAL PAPER

Integrated geoinvestigation for evaluation of an engineering site—a case study from the western Riyadh city, central Saudi Arabia

Sattam A. Almadani[1] · Kamal Abdelrahman[1,2] · Saleh Qaysi[1]

Received: 22 March 2020 / Accepted: 17 February 2021

Abstract

Microtremors were measured at 18 stations to the west of Riyadh, and the H/V spectral ratio method was used to estimate the resonance frequency and amplification factor. These parameters indicate the presence of foundation bedrocks at various levels with variable thickness of soil where resonance frequency varies from 0.26 to 2.63 Hz, while the amplification factor ranges from 1.1 to 8.9. Moreover, four seismic refraction profiles have been carried out and illustrated two layers: the first of which has a P-wave velocity of 2000 m/s and a thickness of 1.5 m, whereas the second layer is characterized by P-wave velocity from 4010 to 4274 m/s. Besides, four multichannel analyses of surface wave (MASW) profiles have been conducted along the same refraction profiles to estimate the shear wave velocities along these profiles. The constructed 1D and 2D models indicate shear wave velocity ranges from 400 m/s to more than 4000 m/s with horizontal and vertical variation through the investigated area. Furthermore, the dynamic properties of rock and soil materials including Poisson's ratio, Young's modulus, shear modulus, material index, concentration index and ultimate bearing capacity have been calculated based on P- and S-wave velocities. These properties reveal less competent to competent material scales. Subsurface karst cavities have been detected in the study area at different depths and various dimensions. It is highly recommended that preventive measures including probing drilling to anticipate karst cavities below the designed foundations must be applied before construction of new engineering facilities in the study area. Otherwise, it will be geotechnical problems in the future.

Keywords Microtremors · MASW · Dynamic properties · Karst cavities · Riyadh · Saudi Arabia

Introduction

Riyadh has witnessed a significant city growth and expansion in recent years. The western part of the city will undergo future extension (Fig. 1) as new urban communities have emerged in this region. Numerous facilities are beginning to appear in this region such as electrical power plants, which demand certain construction and implementation specifications. Therefore, it has become necessary to conduct engineering geological analyses of this region to evaluate its suitability for urban sprawl and the maintenance of important projects in this area. These objectives will be achieved by applying near-surface geophysical methods such as microtremor measurements and seismic refraction and multichannel analysis of surface waves (MASW) (Aldahri et al. 2017, Abdelrahman et al. 2017a, b, 2019). At present, microtremors are used as a fast, widely applicable, and cost-effective site effect assessment method. Moreover, these measurements are able to assess the engineering parameters for the surface soil materials and the foundation bed as well based on the fundamental resonance and amplification factor. Therefore, microtremor measurements have been executed at 18 localities to the west of Riyadh.

The seismic method is a powerful geophysical exploration technique that has been in widespread use in ground engineering for more than 40 years and has been increasingly used since 1996 in geotechnical and environmental applications, usually at depths shallower than 40 m. The applicability of seismic methods depends on the presence of acoustical contrasts in the subsurface. In many cases, the acoustical contrasts

Responsible Editor: Narasimman Sundararajan

✉ Sattam A. Almadani
salmadani@ksu.edu.sa

[1] Geology and Geophysics Department, College of Science, King Saud University, Riyadh, Saudi Arabia

[2] Seismology Department, National Research Institute of Astronomy and Geophysics, Cairo, Egypt

Published online: 26 February 2021

occur at boundaries between geological layers, although man-made boundaries such as tunnels and mines also present contrasts. Seismic survey is the geophysical method, which is most closely related to rock and soil mass properties, since seismic wave velocity varies with the main mechanical properties, such as Poisson's ratios and other modules. The earliest applications of the method primarily concerned the determination of the depth to the bedrock beneath a soil cover. Later, the same method was used successfully for the location of "weak" zones, such as shear zones and faults. Nowadays, seismic methods have been used in connexion with planning of dams (e.g. Klimis).

Furthermore, seismic methods are powerful geophysical exploration techniques that have been used in geotechnical engineering for more than 40 years; they have been increasingly used since 1996 for geotechnical and environmental applications. While recently, MASW becomes a more powerful technique for engineering site evaluation. They are often used for depths of <40 m (Soupios et al. 2015). In many cases, the impedance contrasts occur at the boundaries between geological layers. Seismic surveys are the geophysical method most closely related to rock and soil mass properties because seismic wave velocity varies with major mechanical properties, such as Poisson's ratio and other modulus values. Early applications of seismic methods primarily focused on determining depth to the bedrock beneath soil cover. Subsequently, the same method was used to locate areas of weakness such as cavity karst features, and sinkholes and faults especially in limestones. These karst features are originated due to the seasonal and long-term variations in the groundwater level that may occur because of changes in local and regional groundwater abstraction and recharge.

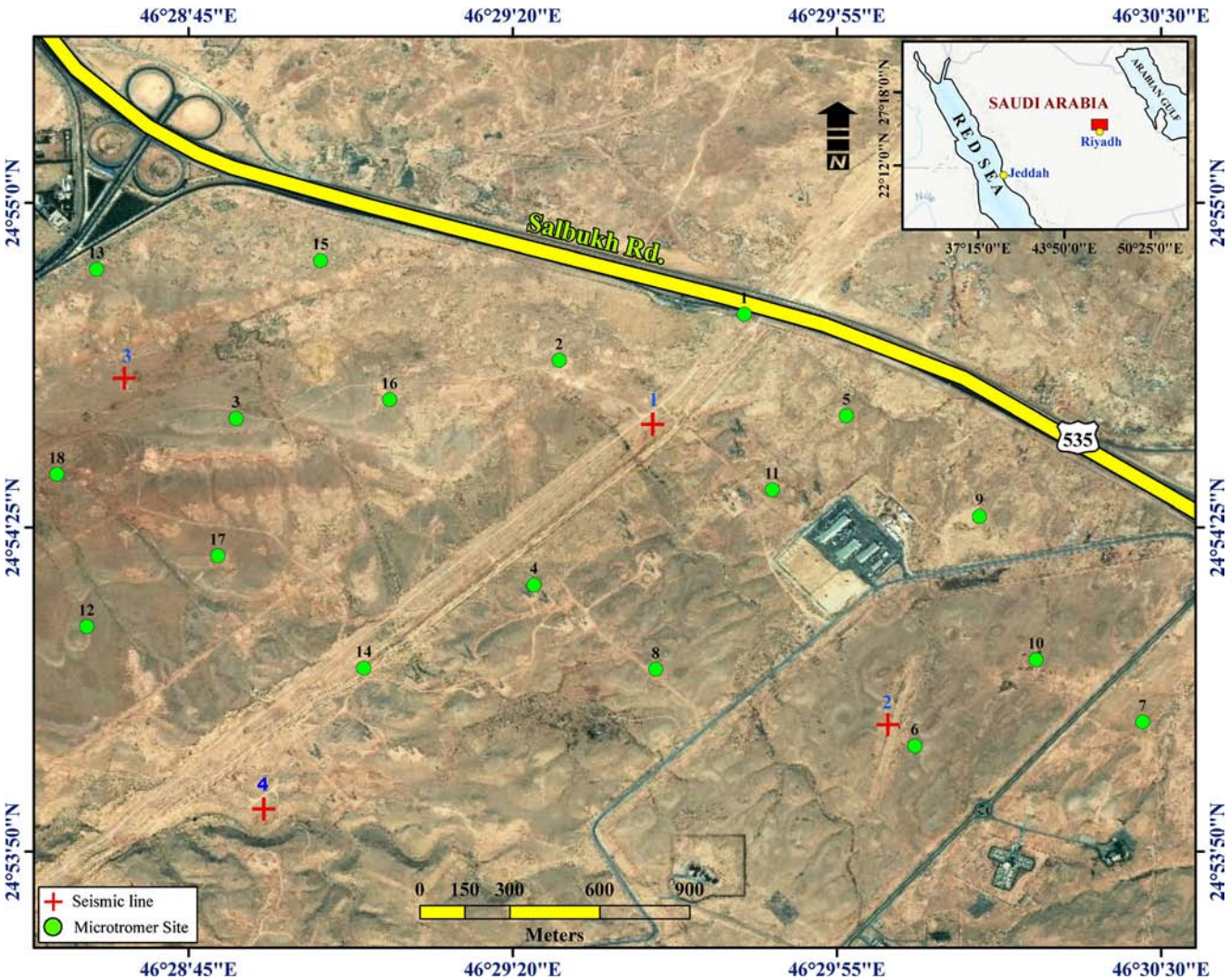

Fig. 1 Location map of the study area, locations of microtremor sites and seismic refraction and MASW field survey

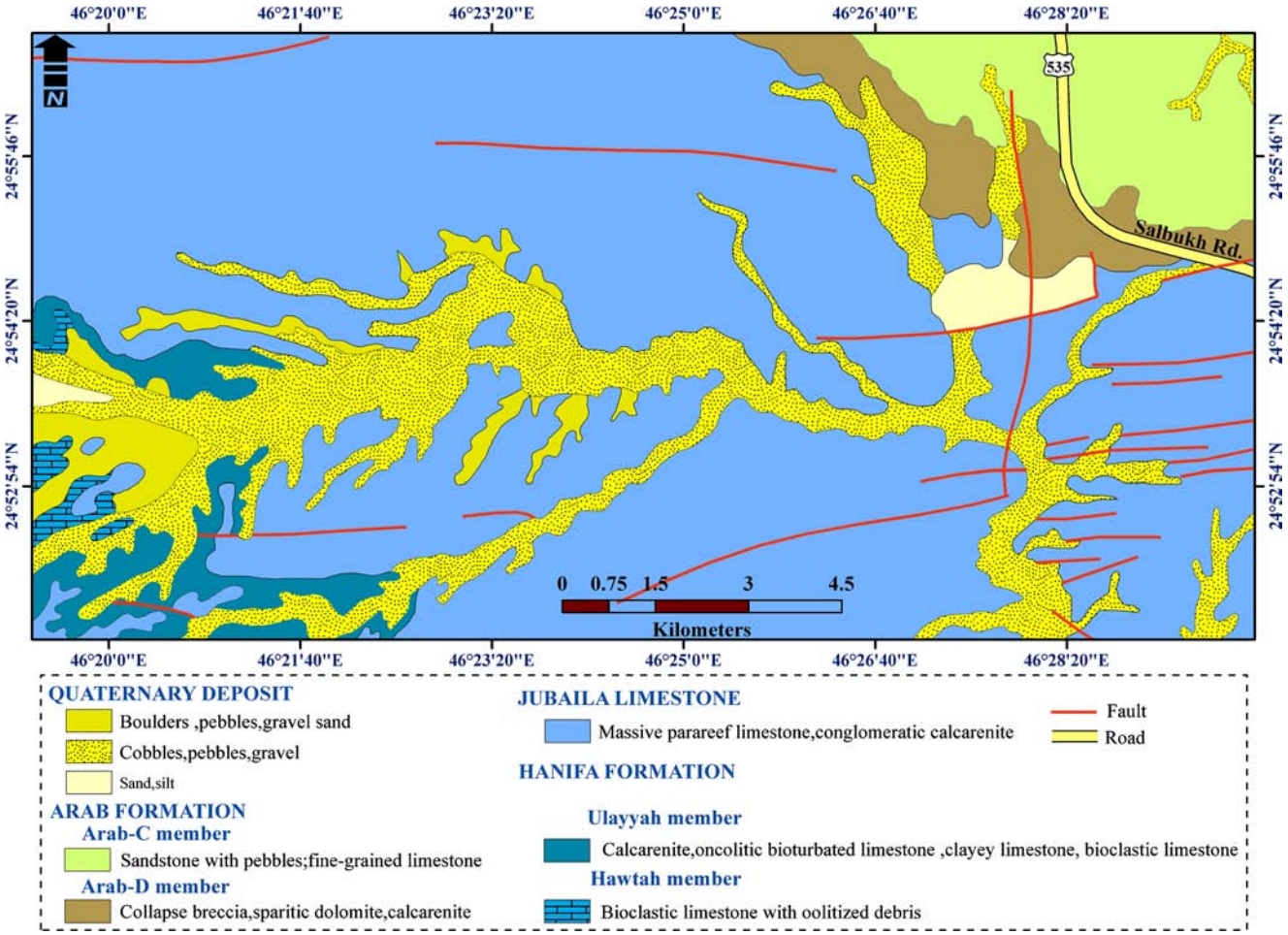

Fig. 2 Geological map for the area of interest

Geological setting

The sedimentary rocks forming the Arabian platform comprise a thick sequence (>2 km below Riyadh) of shallow marine basin deposits, primarily carbonate and siliclastic deposits with intermittent evaporites (Le Nindre et al. 1990). In the vicinity of Riyadh, these strata are dominated by Jurassic (145–200 Ma) and Cretaceous

Table 1 The equations used to estimate elastic properties and material competence scales of soil and rocks in the study area. Where **ν** is Poisson's ratio, V_p is the P-wave velocity, V_s is the shear wave velocity and ρ is the material density

Item	Parameter	Formula
Elastic properties	Stress ratio (S_i)	$Si=\nu/(1-\nu)$
	Poisson's ratio	$\nu=\frac{V_P^2-2V_S^2}{2\left(V_P^2-V_S^2\right)}$
	Young's modulus (E)	$E=\rho\frac{3V_P^2-4V_S^2}{\left(V_P^2-V_S^2\right)}V_S^2$
	Shear modulus (G)	$G=\rho V_S^2$
	Bulk modulus (k)	$B=\rho\left(V_P^2-\frac{4}{3}V_S^2\right)$
Competence scales	Material index (M_i)	$Mi=(1-4\ \nu)$
	Concentration index (C_i)	$Ci=(1+\nu)/\nu$ or $Ci=(3-4\ \alpha)/(1-2\ \alpha)$
	Foundation material bearing capacity (Q_{ult})	Log Qult=2.932 (log Vs−1.45)

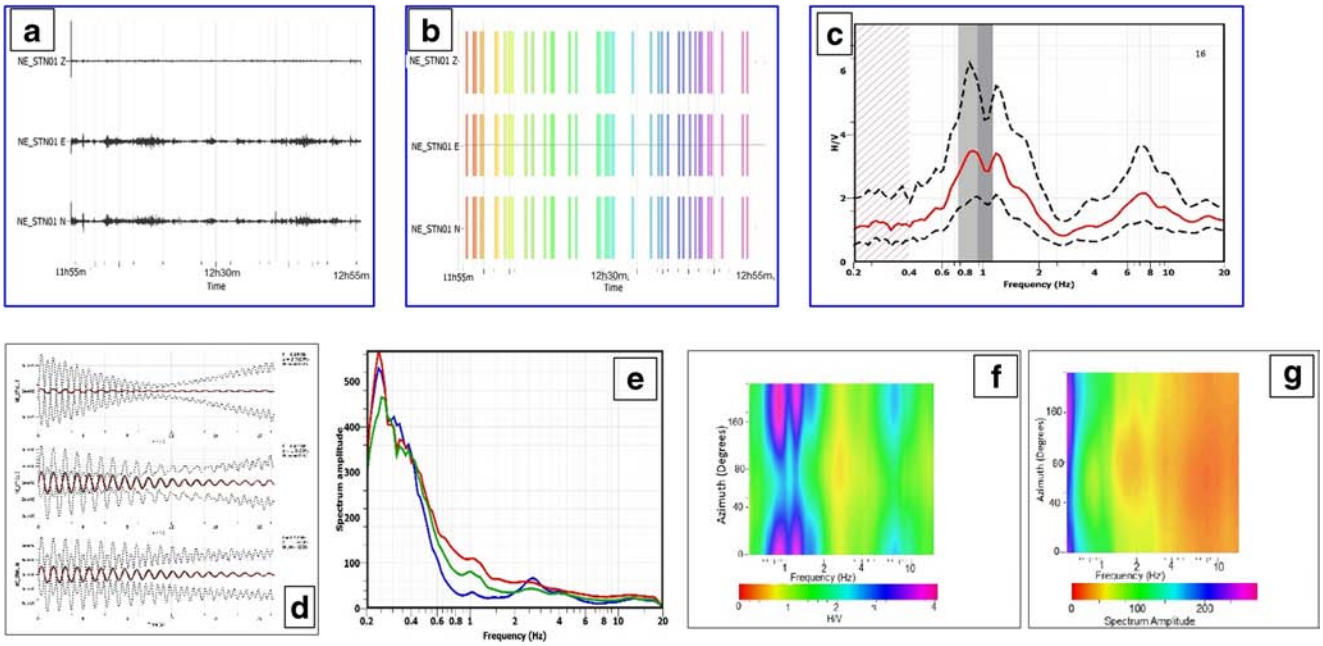

Fig. 3 **a**–**g** Processing sequence of microtremor data

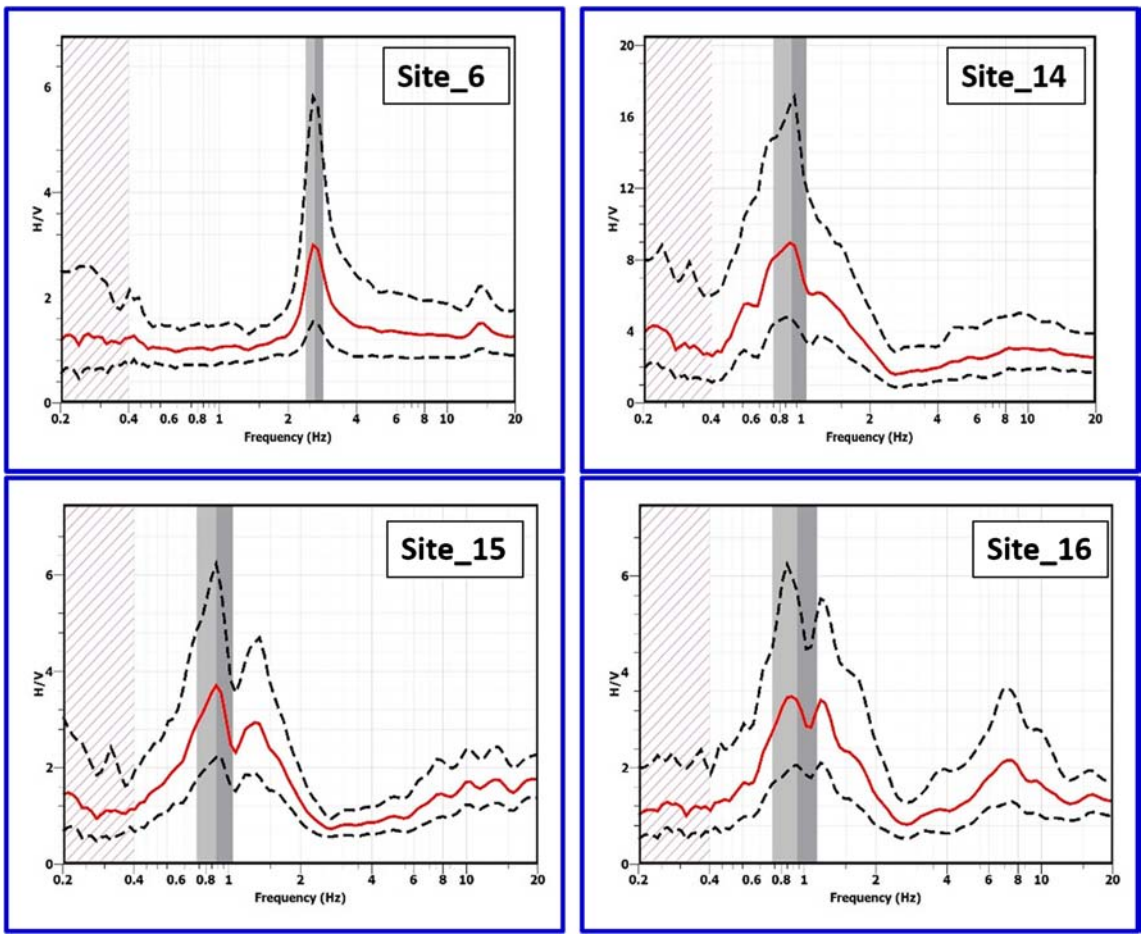

Fig. 4 Examples of H/V of some selected microtremor stations

Table 2 Results of the microtremor data measurements

Station	No. of samples	Windows		Fundamental frequency		H/V peak		Reliable H/V peak							Vulnerability index
		Window length	No. of windows	F_o	STD	A_o	STD	ÕA(f)<2	A_o>2	F-<A_o/2	F+<A_o/2	Õf<E (F_o)	ÕA<(F_o)	$A(F)$±sA=($F0$)±5%	
1	360,000	25	135	0.26	0.03	1.1	2.03	No	No	Yes	Yes	Yes	Yes	Yes	4.653846
2	360,000	25	140	0.29	0.04	1.2	1.79	Yes	No	Yes	Yes	Yes	Yes	Yes	4.965517
3	360,000	25	143	2.61	0.33	1.31	1.22	Yes	No	Yes	No	Yes	No	Yes	0.65751
4	360,000	25	127	2.58	0.22	1.79	1.43	Yes	No	Yes	No	Yes	Yes	Yes	1.241899
5	360,000	25	91	2.63	0.23	2.96	1.94	Yes	Yes	No	No	Yes	Yes	Yes	3.331407
6	360,000	25	110	2.57	0.12	3.14	1.53	Yes	Yes	No	No	Yes	Yes	Yes	3.83642
7	360,000	25	138	0.63	0.07	1.21	1.75	Yes	No	Yes	Yes	Yes	No	Yes	4.066944
8	360,000	25	62	0.83	0.17	4.1	2.51	No	Yes	Yes	Yes	Yes	No	Yes	20.25301
9	360,000	25	92	1.03	0.13	1.58	1.42	Yes	No	No	No	Yes	Yes	Yes	2.423689
10	360,000	25	22	0.8	0.14	4.21	3.16	No	Yes	No	Yes	Yes	Yes	Yes	22.15513
11	360,000	25	89	2.12	0.34	2	1.49	Yes	Yes	Yes	No	Yes	No	Yes	1.886792
12	360,000	25	38	0.89	0.14	8.9	1.88	Yes	Yes	Yes	No	Yes	Yes	Yes	89
13	360,000	25	52	0.88	0.15	3.7	1.67	Yes	Yes	No	No	Yes	Yes	Yes	15.55682
14	360,000	25	39	0.94	0.2	3.39	1.66	Yes	Yes	No	Yes	Yes	Yes	Yes	12.22564

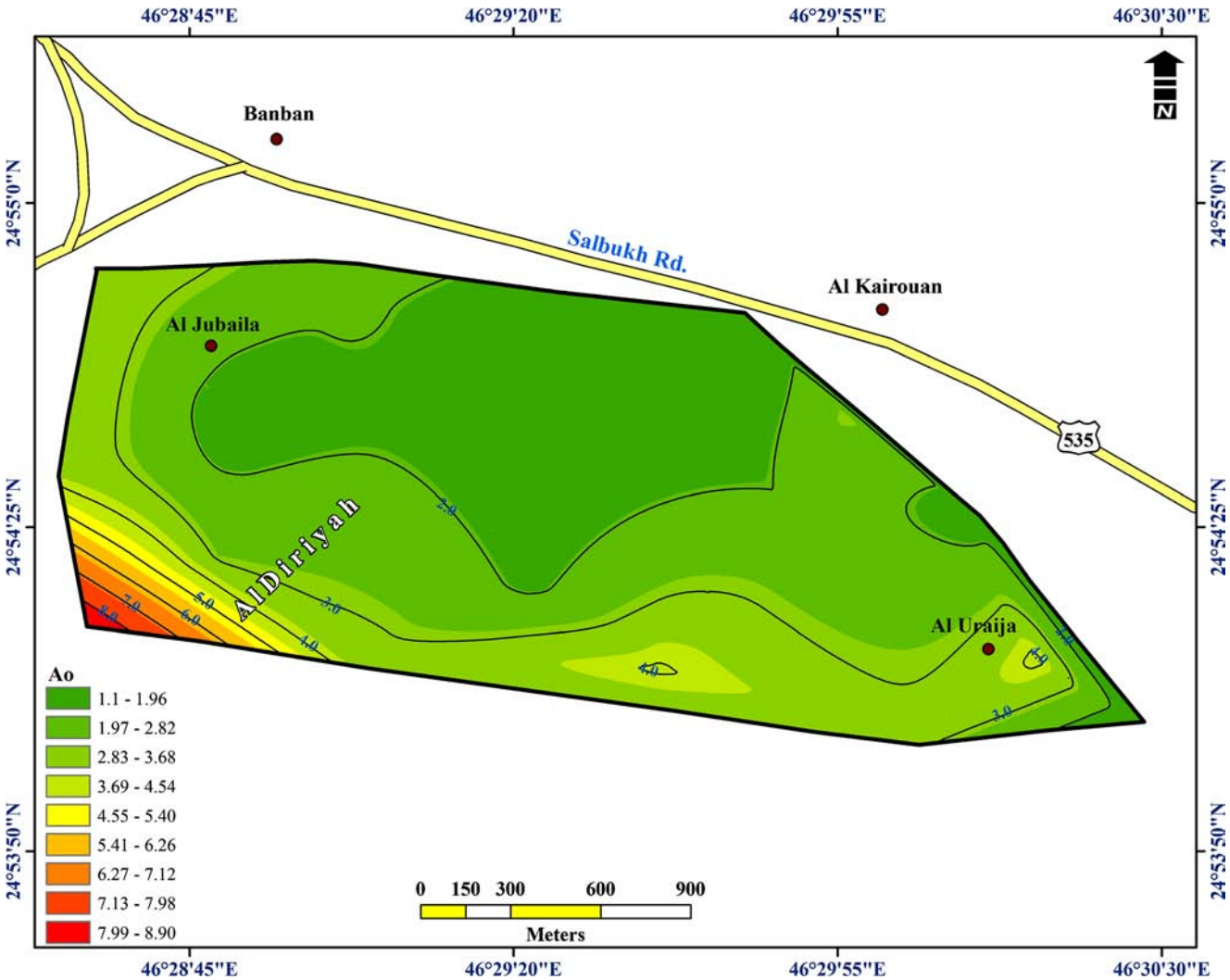

Fig. 5 Distribution of amplification factor through the area of study

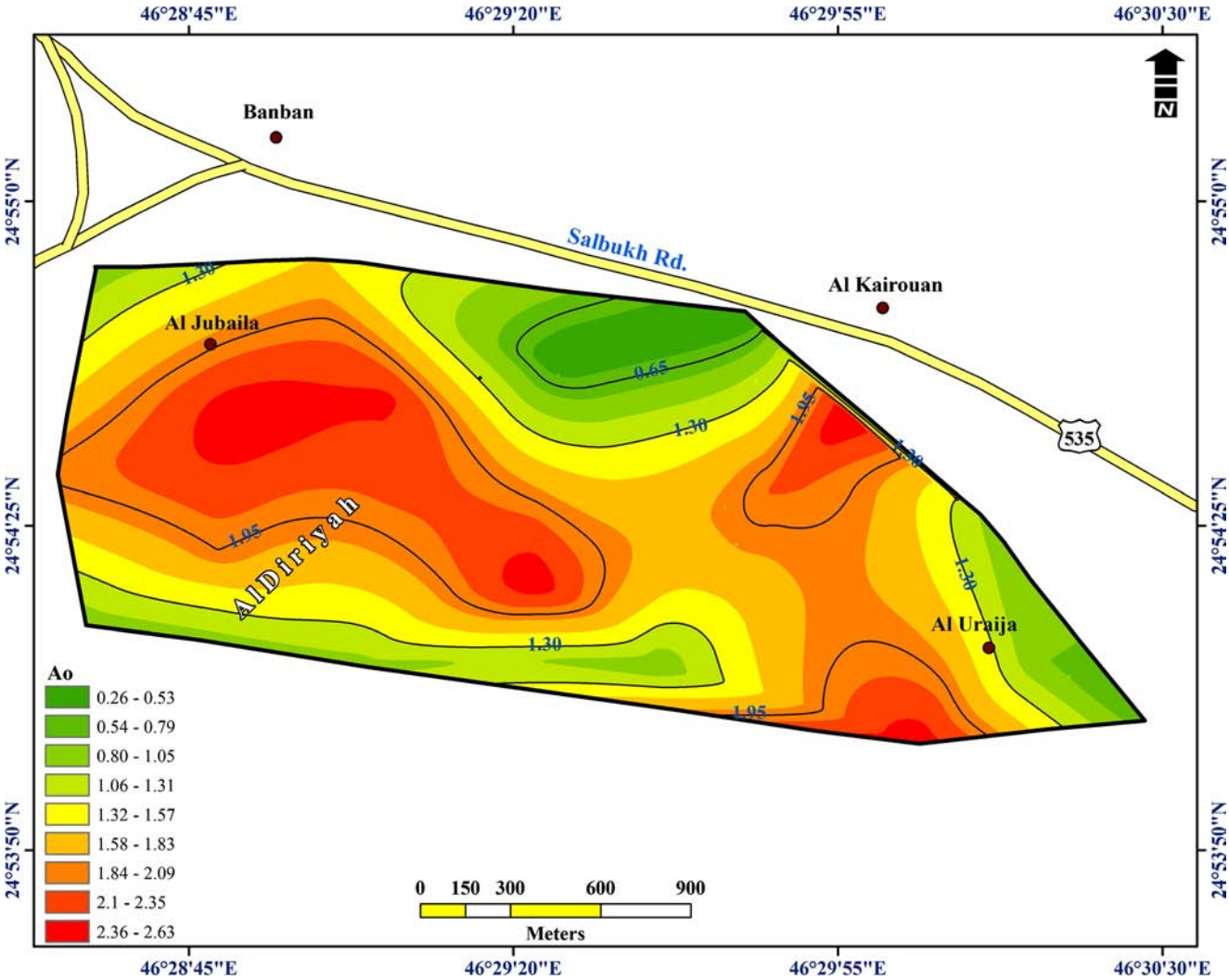

Fig. 6 Distribution of fundamental frequency through the area of study

(65–145 Ma) sedimentary rocks, predominantly marine limestones, claystones and marls (calcareous mudstones). These sedimentary rocks can form aquifers, some of which are used by Riyadh. Generally, the Arabian platform has been incised by southward-flowing seasonal streams forming a series of channels and plateaus. These wadi channels are filled with predominantly unconsolidated, weakly cemented, alluvial deposits of silts and sands that can form fresh to brackish shallow unconfined aquifers.

Riyadh city is established over soluble Mesozoic-Cainozoic sedimentary rocks with a wide variety of karst cavities recorded in numerous sites constituting one of the most important geohazards in the Arabian platform (Al-Refeai and Al-Ghamdy 1994; Amin and Bankher 1997). Vaslet et al. (1991) described the Jurassic to Early Cretaceous rocks (Fig. 2) that outcrop through the Riyadh area. The Jubaila Formation extends several kilometres west of Riyadh city and close to the Jubaila Village. This formation has a stratigraphic extent of 118.3 m (in the type section) and is composed of partially dolomitised aphanitic limestones in the lower 85 m and calcarenitic limestones in the upper 33 m. It is described as a sequence of medium strong to strong (depending on the weathering), dark grey, and pale grey, mud-rich and grain-rich carbonate rocks. The Jubaila Formation is divided into two units; the lower unit (J1) is predominantly composed of compacted limestone with a thickness of ~56 m; the upper unit (J2) is 60-m-thick and more compacted. Moreover, it shows intercalations of grey limestone organic materials.

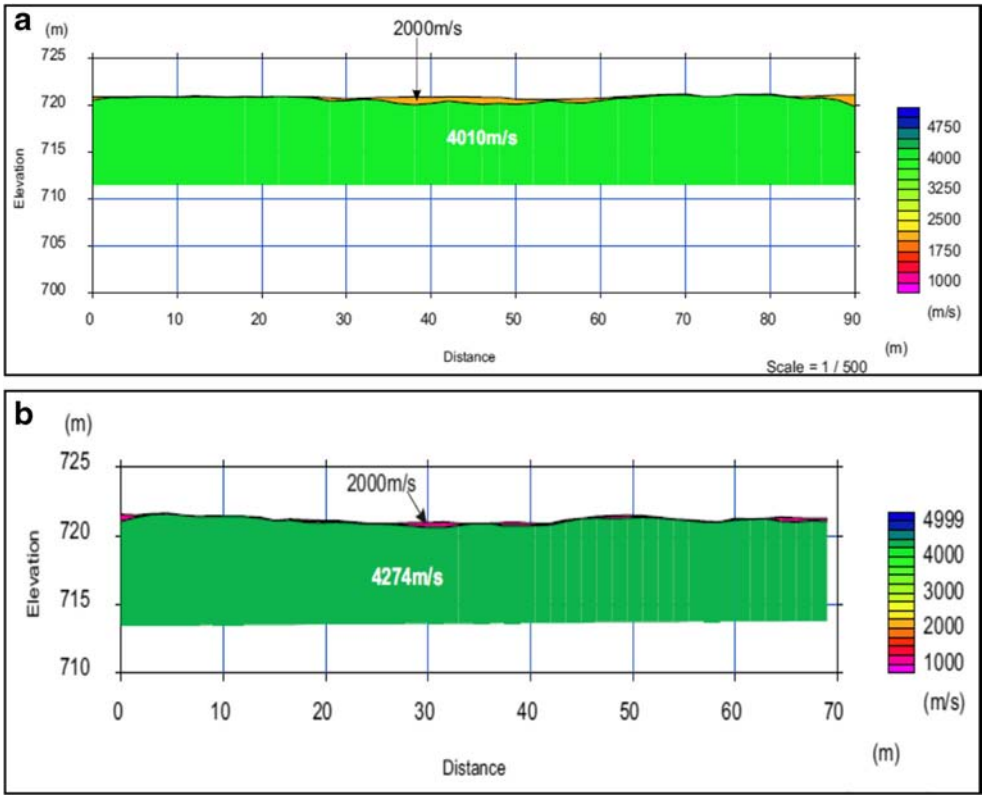

Fig. 7 **a**, **b** Geoseismic cross-sections underneath profiles 1 and 2 and based on P-wave velocities

Methodology

Microtremors are ground vibrations with displacement amplitudes of ~1–10 μm, and velocity amplitudes of 0.001–0.01 cm/s. Many researchers have used microtremors for engineering site evaluation (Nakamura 1989; Singh 2015; Mundepi et al. 2015; Pilz et al. 2014; Panzera et al. 2013a, b; Matassoni et al. 2015). The ratio between horizontal and vertical motions for each observation point is related to soil conditions. Moreover, the horizontal component of the shear wave is amplified by a layer of soft soil because of the multiple reflection phenomena of waves while soft soil layers do not amplify the vertical component (Nakamura 1989; Milana et al. 2011; Choobbasti et al. 2014; Rao et al. 2011).

Furthermore, seismic methods have emerged as powerful tools for computing the elastic moduli from which elastic deformation can be estimated (Stumpel et al. 1984). The reliability of rock or soil materials for foundation purposes is a qualitative term that can be estimated by the average line method (Sjogren et al. 1979; Abd El Rahman and Abd El Latif 1990), such that weak zones can be identified. Nevertheless, the classification of the rocks or soils of a given area on the basis of their degree of competence can be recognized using N value, concentration index, stress ratio and allowable bearing capacity (Imai 1975; Abd El Rahman and Abd El Latif 1990; Abd El Rahman et al. 1991). The estimated P- and S-wave velocities in this study are used to compute the elastic constants in an investigated area. Depending on material elastic parameters, seismic measurements for parameters, such as density (ρ), stress ratio (S_i), Poisson's ratio (ν), rigidity modulus (μ), Young's modulus (E) and bulk modulus (B), have been calculated based on the equations shown in Table 1 to evaluate the foundation layer for civil engineering purposes and rock mass quality.

Data collection and analysis

Microtremor data were obtained for 18 sites to the west of Riyadh (Fig. 1) during September 2019 following the recommendations of the European SESAME research project. For reducing the effect of noise sources that may interfere with the signal, recordings were performed between 10 pm and 6 am. A Taurus digital seismograph was used with a three-component velocity sensor unit of Trillium compact seismometers. Measurements continued for 60 min, with a sampling rate of 100 Hz for every site.

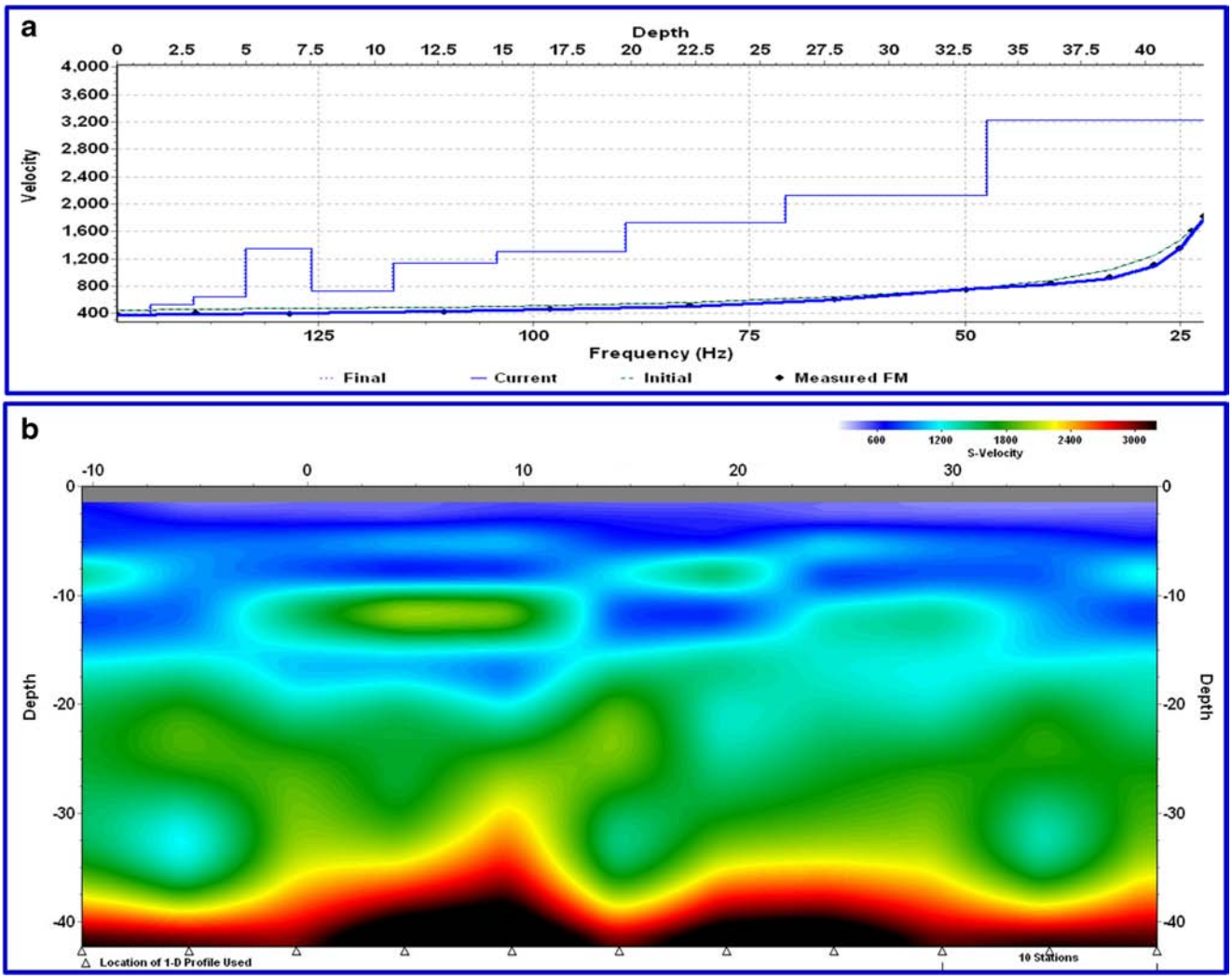

Fig. 9 **a**, **b** 1- and 2D shear wave velocity models along profile 3

Appropriate windows of data were selected from the 50 windows obtained at each site, avoiding windows influenced by proximal noisy sources. Each window is tapered with the Konno-Ohmachi algorithm and filtered from 0.2 to 20 Hz. Fourier spectra were obtained for the selected windows using the fast Fourier transform (FFT) algorithm.

After obtaining the H/V spectra for specific windows, an average spectrum was obtained and used as the H/V spectrum for a particular site. For this purpose, researchers used the SESAME guidelines (http://sesame-fp5.obs.ujf-grenoble.fr, SESAME Project 2004). H/V spectral ratios for selected windows were computed at 16 surveyed sites. Figures 3 and 4 show the analytical procedures and H/V spectral ratio for stations 06, 14, 15 and 16. Table 1 shows the analytical results for all recording stations.

Four seismic refraction profiles were conducted (Fig. 1) using multiple channels signal enhancement seismograph of Geode-model with 48 channels. These profiles have different geophone spacing such that the distance between the shot-point, and the first geophone was 2 m for profile 1 and 1.5 m for profile 2. The data files include the precise positions of each geophone and the shot point as measured by the synchronized GPS instrument in the field. Furthermore, three shooting points used the forward, the mid-point and the reverse shooting technique. Field measurements were acquired using a hydraulic weight drop with 200 kg for generating compressional waves via repeated impacts on a metal striker plate. Moreover, four MASW profiles have been carried out along the same seismic refraction profiles. These data were carried out using vertical geophones of 4.5 Hz that could reach greater depths, of at least 30 m.

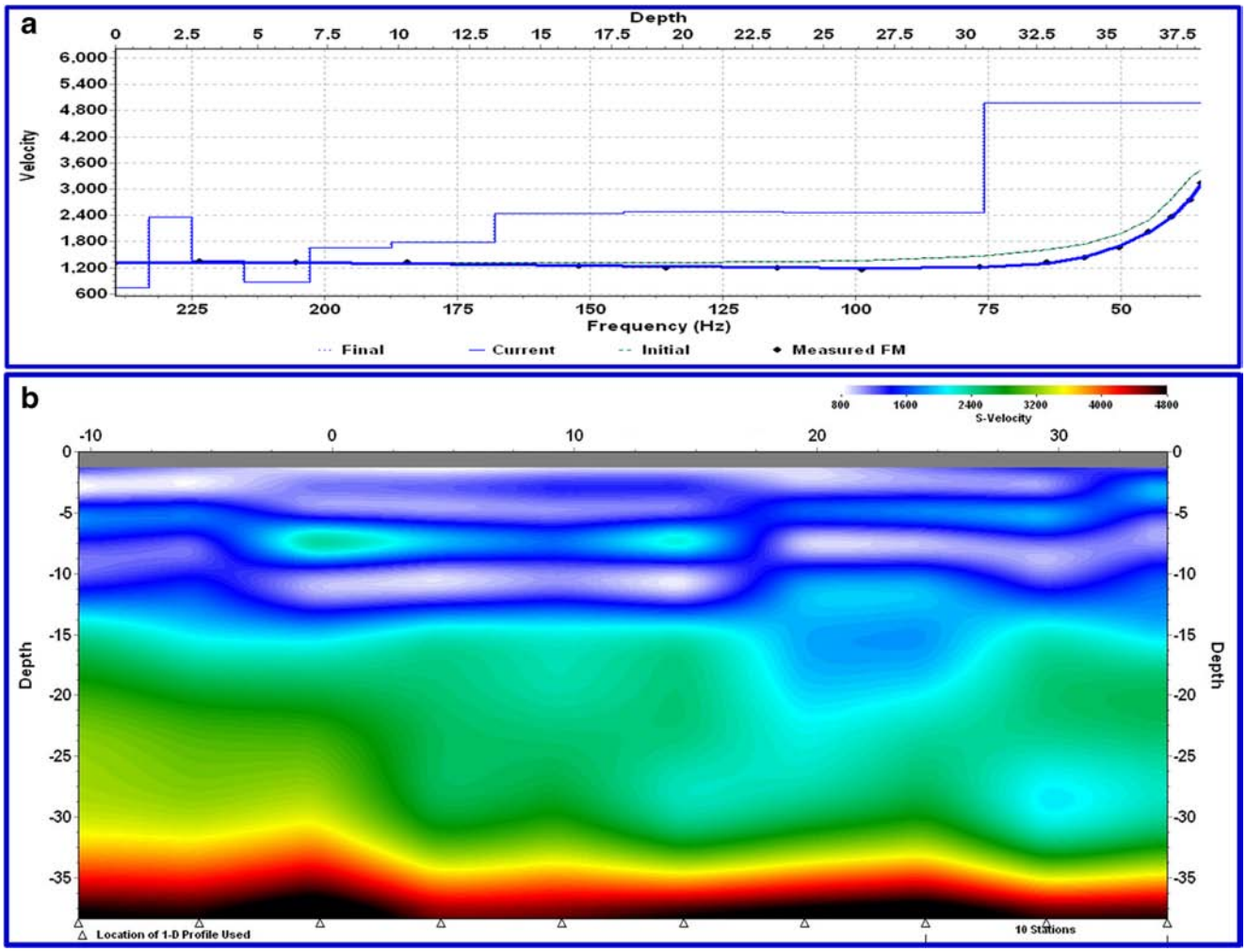

Fig. 8 **a**, **b** 1- and 2D shear wave velocity models along profile 3

Results and discussion

At 18 surveyed stations, the H/V spectral ratios for designated windows were calculated (Table 2). These data displayed the peak frequency $f_{(Peak)}$ varies from 0.26 to 2.63 Hz within the study area and can be sub-classified in two frequency ranges. The first group corresponds to those <1.5 Hz, whereas the second group corresponds to those >1.5 Hz. Most measurements are at higher values of $f_{(Peak)}$ (>1.5 Hz, i.e. ~80%), indicating a small thickness of sediments. Furthermore, the amplification factor ranges from 1.1 up to 8.9, where it can be categorized into two groups, i.e. those <2.0 and those >2.0 (~60%). Figure 5 shows the distribution of peak frequencies for the study area, where the majority show a peak frequency greater than 1.5 Hz. The central part is characterized by higher

Table 3 Ranges of concentration index and stress ratio correspondent to the soil competent degree (after Abd El Rahman 1989)

	Weak		Fair		Good
	Incompetent		Fairly competent		Competent
	Very soft	Soft	Fairly compacted	Moderate compacted	Compacted
Concentration index	3.5–4.0	4.0–4.5	4.5–5.0	5.0–5.5	5.5–6.0
Stress ratio	0.7–0.61	0.61–.52	0.52–0.43	0.43–0.34	0.34–0.25

Table 4 Poisson's ratio (ν), rigidity (μ) and material index (M_i) correspondent to different materials (after Birch 1966)

Rock sample	ν	μ	M_i
Liquids	0.5	0	−1
Perfect elastic rocks	0.25	$\mu=\lambda$	0
Very hard indurated rocks	0.00	$\lambda=0$	+1

peak frequency values (>1.5 Hz) while the residual part of the map shows the frequencies below 1.5 Hz. Figure 6 displays the variation of the amplification factor (H/V amplitude) where the major part of the study area is shown to have lower amplification (<2.0), while the higher amplification factor recorded at sites limited number of stations reflecting greater thicknesses of alluvium sediments or highly weathered limestone rocks.

The acquired seismic refraction data was processed using the *SeisImager of Geometrics* Company software (Fig. 7). The first arrivals were identified at each channel and subjected to processing, beginning with elevation correction to the ground datum. The waveforms were filtered to eliminate high-frequency noise. Figure 9 show the analysis sequences of seismic refraction data for P-wave velocities in profiles 1 and 2 for examples. Profile 1 has a length of 94 m, including 48 geophones with a geophone interval of 2 m. The first arrivals of P-waves were used to construct travel time-distance curves based on observed and calculated travel time-distance curves. The resulting geoseismic ground model indicates two layers (Fig. 9a). The average thickness of the surface layer reaches ~0.5 m with P-wave velocity of 2000 m/s. This layer is composed of weathered limestone and has a very limited extension. The second layer composed of hard limestone with a P-wave velocity of 4010 m/s. This layer represents the primary bedrock at the study area.

Profile 2 is 70.5 m long and contains 48 geophones with a 1.5-m geophone spacing. The first arrivals of P-waves and the recorded seismograms show observed and calculated travel time-distance curves, and the ground model constructed is shown in Fig. 9b. The first layer is very thin, with a maximum thickness of ~0.2 m with P-wave velocity of 2000 m/s. This layer is constituted of clayey sand and gravel while the second layer has P-wave velocities of 4274 m/s and composed of hard limestone.

There are two low-velocity zones at depths of approximately 5 m and 15 m. Figure 8 illustrates 1- and 2D ground models along profile 3. This ground model indicates the range of shear wave velocity ranges 550 to 4850 m/s and extends down to 37.5 m depth. The surface soil extends to a depth of 1.25 m whereas low-velocity zone recorded between 3.5 and 7.0 m depth. Figure 9 shows 1- and 2D shear wave velocity model extends down to more than 40 m depth while the velocity varies between 400 and 3250 m/s. The surface soil layer extends to a depth of 5 m below the ground surface (where V_s is less 800 m/s). It is noticed that there are low-velocity zones between 7.25 and 10.8 m depth below the surface of the earth.

The density gradient in the study area ranges from 2.46 to 2.5 gm/cm^3 for the limestone bedrock, indicating compacted rock (Tables 3, 4 and 5). The study area has a stress ratio of 0.27, indicating competent and compacted rock as per Tables 3, 4 and 5. The Poisson's ratio, ν, at the study site, is 0.21 for the bedrock, indicating competent (hard) rocks. The Young's modulus (E) at the study area varies from 3.49 to 4.02×10^{11}, again indicating competent and compacted rock. The values of shear modulus (G) and bulk modulus (B) in the study area range from 1.434 to 1.653×10^{11} and from 2.053 to 2.372×10^{11}, respectively, once again indicating compacted rock.

Rocks and soil materials competence scales including material index (M_i), concentration index (C_i) and ultimate bearing capacity (Q_{ult}) have been calculated based on measurements of P- and S-wave velocities. The values of M_i range from 0.129 to 0.132, suggesting competent materials (Tables 3, 4 and 5). Concentration index (C_i) varies from 5.59 to 5.61, suggesting a competent and compacted rock. The foundation material bearing capacity (Q_{ult}) in the study area varies from 462.59 to 556.58 kg/cm^2 for the bedrock layer indicating compacted rock (Tables 3, 4 and 5).

Table 5 Soil description with respect to Poisson's ratio (ν) and material index (M_i) (after Birch 1966)

Soil description parameters	Incompetent to slightly competent	Fairly to moderately competent	Competent materials	Very high competent materials
Poisson's ratio	0.4–0.49	0.35–0.27	0.25–0.16	0.12–0.03
Material index	(−0.5)–(−1)	(−0.5)–(0.0)	0.0–0.5	> 0.5

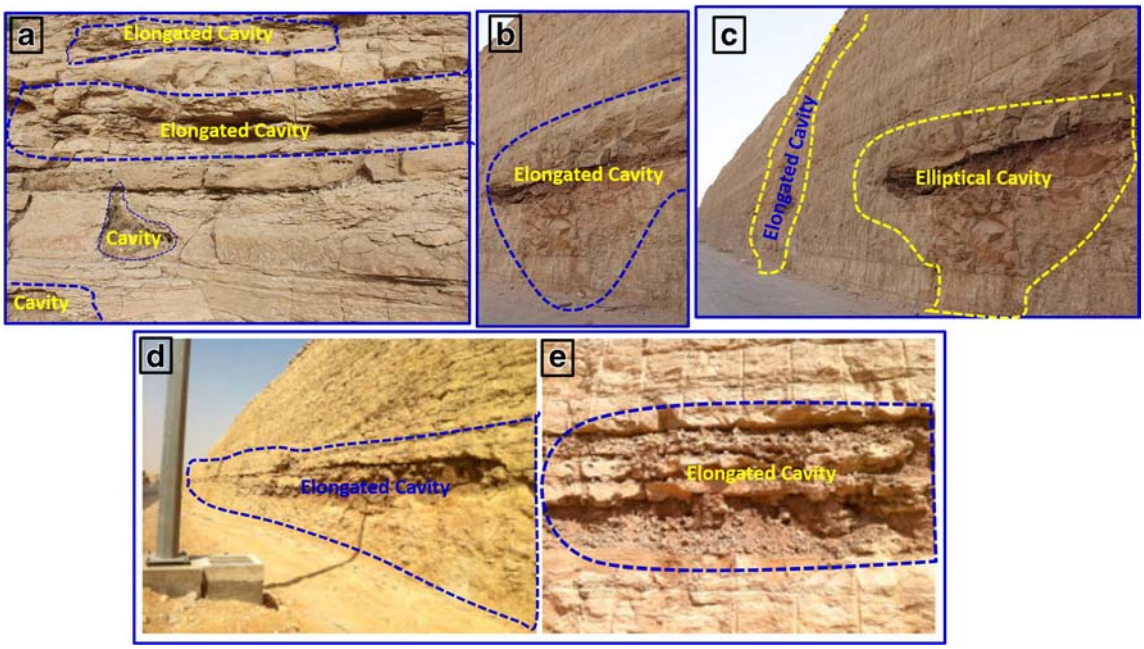

Fig. 10 **a**–**e** Cavity features of Jubaila limestones in the area of study

Conclusions

In this study, site response effect and site soil characteristics have been assessed for western Riyadh. There is a wide range of resonance frequency of 0.26–2.63 Hz while the corresponding amplification factor varies between 1.1 and 8.9. The sharp peaks indicate the impedance contrast between the uppermost surface soil and the underlying hard rock (SESAME Project 2004). These second peaks reflect large impedance contrasts (SESAME Project 2004). Other sites present broad peak curves, which could be related to the presence of a subsurface sloping interface between softer and harder layers (SESAME Project 2004; Fnais et al. 2010).

Moreover, seismic refraction illustrates two layers; the first layer has P-wave velocities of ~2000 m/s and represents the Quaternary deposits (<2.6 Ma) at the site of interest, which are likely loose to dense interbedded alluvium and composed of red-brown clay, silt, and sand. Aeolian deposits composed of thinly laminated and gently inclined fine sand and coarse silt are present. This layer has a thickness of 1.5 m. Whereas, the second layer possesses of P-wave velocities ranging between 4310 and 4720 m/s and composed of slightly to moderately weathered limestone which, in turn, represents the main bedrock at the study area. Based on the MASW results, Figs. 10, 11, 12 and 13 indicate a low-velocity zone at depth of 15 m, at a depth of approximately 5 m as well as at a depth of 15 m and at depth ranges from 3.5 to 7.0 m and between depths of 7.25 and 10.8 m, respectively.

In conclusion, the Jubaila Formation has possibilities to create subsurface cavities (low-velocity zones), and this is illustrated in Fig. 10, which displays several karst cavities at different depths and with different dimensions. There are several geohazards due to karst generation as follows: (1) the presence of undetected voids and infilled cavities; (2) the uncontrolled and potentially significant groundwater ingress during construction, connected voids could be potential pathways for uncontrolled water inflow; and (3) the existing joints may be enlarged because of dissolution and may result in secondary fissuring. Finally, these low-velocity zones (cavities) have been detected and localized through MASW investigation. These low-velocity zones have to be explored and avoided during land-use planning.

Acknowledgements The authors would like to extend their sincere appreciation to the Deanship of Scientific Research at King Saud University for funding this research group No. RGP -1436-010.

Declarations

Conflict of interest The author(s) declare that they have no competing interests.

References

Abd El Rahman M (1989) Evaluation of the kinetic moduli of the surface materials and application to engineering geologic maps at Ma'Barrisabah area (Dhamar province). Western Yemen Egypt J Geol 33(1-2):229–250

Abd El Rahman M, Abd El Latif T (1990) Geophysical interpretations for shallow engineering site investigations at the area north of Sana'a, Yemen Arab Republic. MERC 4:41–51

Abd El Rahman M, Setto I, El Werr A, 1991.Seismic refraction interpretation for shallow engineering site investigations at the distinctive district 6th of October City. E.G.S. Proc. of the 9th Ann. Meet., 229–242

Abdelrahman K, Al-Amri A, Al-Arifi N, Abdelmoneim E (2017a) Seismic risk assessment at the proposed site of Gemsa Wind Power Station, south-western coast of Gulf of Suez, Egypt. J Geol Soc India 89(February 2017):192–196

Abdelrahman K, Fnais M, Enayat A, Khaled M, Saadoon AB (2017b) Seismic vulnerability assessment in the new urban area of Diriyah Governorate, Riyadh, Saudi Arabia. Arab J Geosci 10:434. https://doi.org/10.1007/s12517-017-3222-7

Abdelrahman K, Abdullah A-A, Al-Otaibi N, Fnais M, Abdelmonem E (2019) Ground motion acceleration and response spectra of Al-Mashair area, Makkah Al-Mukarramah, Saudi Arabia. Arab J Geosci 12:346. https://doi.org/10.1007/s12517-019-4526-6

Aldahri M, Morgen S, Kamal Abdelrahman, Zahran H, El Hady Sh, El-Hadidy M, 2017. Surface soil assessment in the Ubhur area, north of Jeddah, western Saudi Arabia, using a multichannel analysis of surface waves method. Journal Geological Society of India, Vol.89, April 2017, Pp

Al-Refeai T, Al-Ghamdy D (1994) Geological and geotechnical aspects of Saudi Arabia. Geotech Geol Eng 12:253–276

Amin AA, Bankher KA (1997) Karst hazard assessment of eastern Saudi Arabia. Nat Hazards 15:21–30

Birch F (1966) Handbook of physical constants. Geol Soc Amer Men 97: 613

Choobbasti AJ, Rezaei S, Farrokhzad F, Azar PH (2014) Evaluation of site response characteristics using nonlinear method (case study: Riyadh, Iran). Front Struct Civ Eng 8(1):69–82

Fnais MS, Abd El Rahman K, Al-Amri AM (2010) Microtremor measurements in Yanbu city of western Saudi Arabia: a tool for seismic microzonation. J King Saud Univ 22:97–110

Imai S (1975) An investigation to geophysical prospecting for civil purposes. OYO Corporation, Tokyo, Japan

Le Nindre Y-M, Manivit J, Manivit H, Vaslet D, 1990. Sequential stratigraphy of the Central Saudi Arabian platform in the Jurassic and Cretaceous. Ministry of Petroleum and Mineral Resources, Directorate General of Mineral Resources, Jeddah, Saudi Arabia, Technical Report BRGM-TR-11-4, 11

Matassoni L, Fiaschi A, Silengo MC, Lotti A, Saccorotti G (2015) Preliminary seismic microzonation in a mountain municipality of Tuscany (Italy). Open Geosci 7:559–571

Milana G, Azzara RM, Bertrand E, Bordoni P, Cara F, Cogliano R, Cultrera G, Di Giulio G, Duval AM, Fodarella A, Marcucci S, Puccilo S, Regnier J, Riccio G (2011) The contribution of seismic data in microzonation studies for downtown L'Aquila. B Earthq Eng 9:741–759

Mundepi AK, Galiana-Merino JJ, Asthana AKL, Rosa-Cintas S (2015) Soil characterisations in Doon Valley (north west Himalaya, India) by inversion of H/V spectral ratios from ambient noise measurements. Soil Dyn Earthq Eng 77:309–320

Nakamura Y (1989) A method for dynamic characteristics estimation of subsurface using microtremor on the ground surface. Q Rep RTRI 30:25–33

Panzera F, D'Amico S, Lotteri A, Galea P, Lombardo G (2013a) Seismic site response of unstable steep slope using noise measurements: the case study of Xemxija Bay area. Malta Nat Hazards Earth Syst Sci 12:3421–3431

Panzera F, D'Amico S, Galea P, Lombardo G, Gallipoli MR, Pace S (2013b) Geophysical measurements for site response investigation: preliminary results on the island of Malta. Boll Geofis Teor Appl 54: 111–128

Pilz M, Parolai S, Bindi D, Saponaro A, Abdybachaev U (2014) Combining seismic noise techniques for landslide characterisation. Pure Appl Geophys 171:1729–1745

Rao NP, Kumar MR, Seshunarayana T, Shukla AK, Suresh G, Pandey Y, Raju RD, Pimprikar SD, Das C, Gahalaut K, Mishra PS (2011) Site amplification studies toward seismic microzonation in Jabalpur urban area, central India. Phys Chem Earth 36:1247–1258

SESAME Project (2004) Site effects using ambient excitations. http://sesame-fp5.obs.ujf-grenoble.fr

Singh AP (2015) Seismic hazard evaluation in Anjar city area of western India: microtremor array measurement. Soil Dyn Earthq Eng 71: 143–150

Sjogren B, Ofsthus A, Sandberg J (1979) Seismic classification of rock mass qualities. Geophys Prospect 27:10–40

Soupios PM, Papazachos CB, Vargemezis G, Fikos I (2015) Application of seismic methods for geotechnical site characterisation. In: International Workshop in Geoenvironment and Geotechnics, September 2005. Greece, Milos island

Stumpel H, Kaehler S, Meissner R, Milkeret B (1984) The use of seismic shear waves and compressional waves for lithological problems of shallow sediments. Geophys Prospect 32:662–675

Vaslet D, Al-Muallem MS, Maddah SS, Brosse JM, Fourniguet J, Breton JP, Le Nindre YM, 1991. Geologic map of the Ar Riyad quadrangle, sheet 241, Kingdom of Saudi Arabia (with text): Saudi Arabian Directorate General of Mineral Resources, Jeddah, Geosciences Map, GM- 121A